Model-based Reconstruction of Freeform Surfaces with Radial Basis Functions

Friedrich Fleischmann[1], Tobias Binkele[2], Nils Müller[3], David Hilbig[1]
[1] Hochschule Bremen, 28199 Bremen, Germany
[2] OPTIMARE Systems GmbH, 27572 Bremerhaven, Germany
[3]ATLAS ELEKTRONIK GmbH, 28309 Bremen, Germany
friedrich.fleischmann@hs-bremen.de

Summary:

Optical elements with freeform surfaces open new degrees of freedom in the design of optical systems. Reliable measurement of shape is challenging, specially in case of strongly curved ones. A realization of deflectometry, Experimental Ray Tracing, has proven to measure those surfaces with high accuracy. A crucial step is integration of measured gradients from sampled and noisy data. A model based method for surface reconstruction based on Radial Basis Functions (RBF) using non-linear optimization is presented and compared to a new machine learning based RBF-Network approach.

Keywords: Freeform measurement, Deflectometry, Radial Basis Function (RBF), Radial Basis Function Network (RBFN), Experimental Ray Tracing (ERT)

Background and Motivation

In last decade, freeform surfaces on optical components have proven ability to reduce aberrations, size and weight of imaging and non-imaging optical systems [1]. While specific freeforms like aspheres already are measured with high accuracy, those with strong deviations from spherical or flat shape are still challenging [2,3]. Gradient based measurement techniques measure surface slopes instead of height, reducing complexity of setup and need for high dynamic range of sensor, but demand intensive post processing for surface reconstruction [4,5].

One of those, Experimental Ray Tracing (ERT), determines the direction change of a narrow beam passing an optical element. In previous work, method and setup to realize ERT for measurement of reflective surfaces was introduced and uncertainties were discussed [6].

Method

Here, we present the model-based reconstruction approach used, enforcing integrability and using integration of RBF by non-linear optimization and compare this to a new approach based on RBFNs.

The setup is sketched in *Fig. 1*. For measurement, the incident ray i is directed to the surface under test (SUT) and reflected, with new direction *r* depending on i and surface normal *g* at the point of reflection. Those vectors can be represented by direction vectors, and point of intersection by its position vector. Sampling the area $\boldsymbol{A}$ of SUT, one can derive surface normals in intersection points of area of interest $\boldsymbol{A}$ by

$$\boldsymbol{g} = \frac{\boldsymbol{r} - \boldsymbol{i}}{\sqrt{2(1 - (\boldsymbol{r} \cdot \boldsymbol{i}))}}$$

In *Fig.1*, relevant coordinate systems CS are introduced. Those are the CS of incident ray with the basis $\mathscr{I}$ describing vectors *i* , r, g, the

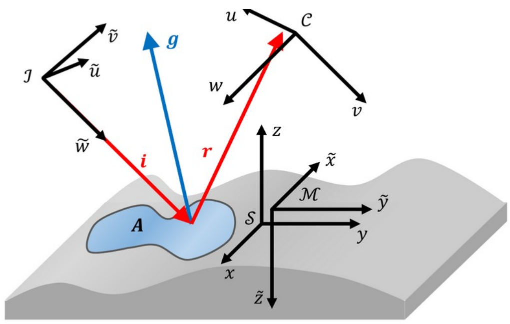

Fig. 1: Symbolic measurement setup. Device under test in grey, investigated area $\boldsymbol{A}$ *in blue. Incident ray* i*, reflected ray r.*

CS Camera $\mathcal{C}$ describing intensity distributions on sensor, CS of Measurement plane $\mathscr{M}$ identifying the direction of the sampling of the SUT, and CS of SUT with the basis $\mathcal{S}$ and axes x, y, z, describing the model function of SUT with height

$z = s(\boldsymbol{x})\colon \mathbb{R}^2 \rightarrow \mathbb{R}$, with $\boldsymbol{x} = (x, y)^T \in \boldsymbol{A}$ (1)

Necessary coordinate transformation between CS is eased by homogeneous coordinates [7].

DOI 10.5162/SMSI2025/B5.1

The surface normals are determined in CS $\mathcal{C}$, resulting in a surface normal at position $\boldsymbol{x}_i$ as $\boldsymbol{g}_i^{\mathcal{C}}$. Having all sample points acquired, normals are transferred into the CS $\mathscr{M}$. From normal's slopes a gradient field in CS $\mathcal{C}$ is derived. For numerical integration, a model of surface using RBS (Wendland functions) is used, with number of RBFs beeing identical to number of sample points and centers located in the measurement positions $\boldsymbol{x}_i$. Derivatives of RBF are fitted to measured gradients. Due to uncertainties and noise, an additional nonlinear optimization step is necessary. Flow of reconstruction process is depicted in *Fig. 2*.

The second method uses supervised learning for reconstruction. A "Growing and Pruning" RBFN was implemented, which uses derivatives of the Wendland function as a basis, see *Fig. 3*. That approach promises a reduction of compute time and memory, since model is optimized continuously by new measurement data.

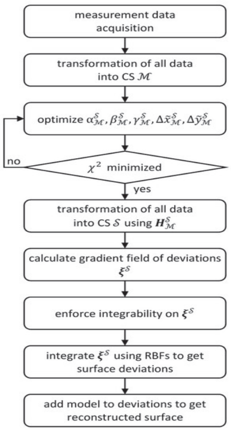

Fig. 2: Flowchart of the reconstruction process.

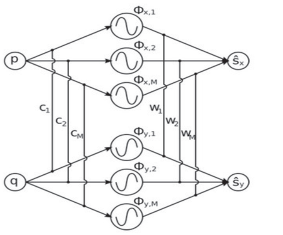

Fig. 3: Schematic Architecture for the RBF Network. Φ_x und Φ_y are derivatives of RBFs in x- and y-direction, c_i denotes i-th center position, p and q are the measured gradients in x and y direction and $\hat{s}$ are the approximated gradients in x and y direction.

Results

The reconstruction methods were applied in simulation as well as in measurement. For comparison reasons, here the outcome of simulated measurement of a "Franke-surface" is presented, see *Fig. 4* and *5*. The surface was evaluated using nonlinear optimization and integration (compare *Fig. 2*) as well as using supervised learning with RBFN approach (*Fig. 3*). Both methods result in extremely small deviations. The optimization method also proved its performance with real live data.

Tab. 1: Comparison of reconstruction performance.

Method	RMS/normalized	t/s
Integration	2.560e-4	126.312
RBFN	8.623e-6	42.583

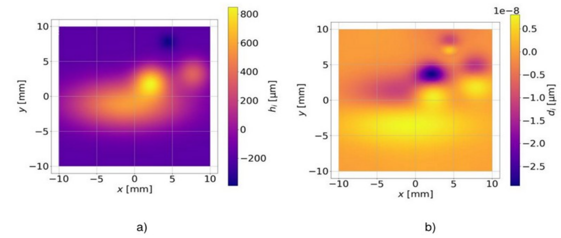

Fig. 4: Plots presenting a) the reconstructed "Franke" surface and b) its deviation from the surface model using RBF integration .

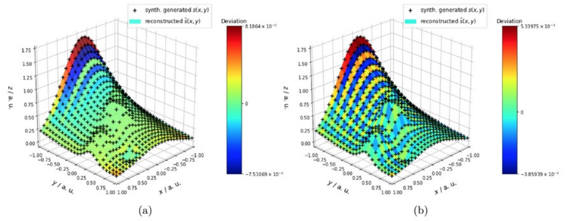

Fig. 5: Comparison of reconstruction using a) least-square RBFN and b) integration of RBF.

Conclusion

Two model-based techniques for reconstruction of freeform surfaces from gradient data are compared. In simulation, data-driven RBFN outperforms integration method especially in regard of processing time, but performance in real measurement has to be investigated further.

References

[1] K. P. Thompson and J. P. Rolland, Freeform Optical Surfaces: A Revolution in Imaging Optical Design, *Optics & Photonics News* 23(6), 30-35, (2012); doi: 10.1364/OPN.23.6.000030

[2] Ines Fortmeier *et al,* Results of round robin form measurements of optical aspheres and freeform surfaces *Meas. Sci. Technol.* **35** 085012 (2024); doi: 10.1088/1361-6501/ad4730

[3] M. Khreishi *et al*, Enabling precision coordinate metrology for universal optical testing and alignment applications, Opt. Eng. 60(3) 035106 (2021)

[4] Wagner, C., Häusler, G., Information theoretical optimization for optical range sensors, Appl. Opt. Vol. 42 No. 27 (2003).

[5] S. Ettl, J. Kaminski, M. C. Knauer and G.Häusler, Shape reconstruction from gradient data, Applied Optics 47, 2091-2097 (2008).

[6] T. Binkele, *et al*, Characterization of specular freeform surfaces from reflected ray directions using experimental ray tracing, *J. Sens. Sens. Syst.*, 10, 261–270 (2021); doi: 10.5194/jsss-10-261-2021.

[7] M. Duncan, Applied Geometry for Computer Graphics and CAD, 2nd edition, Springer, (2005)